COHERENT X-RAYS AND THEIR APPLICATIONS
A series of tutorial–level lectures edited by Malcolm Howells

Lecture 6 - 9th June 2008

Coherence activities at the ESRF:

Scanning (Transmission) X-ray Microscopy

STXM → SXM

A Practical Approach

Jean SUSINI

Scanning X-ray microscope arrangements

- Detection of signals arising from interaction of small probe with sample
- Sample scanned through beam to build 'image' pixel by pixel

Scanning Transmission X-ray Microscope

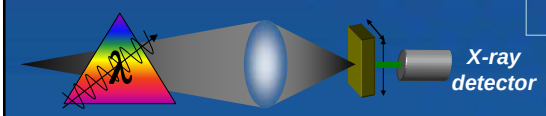

- Soft- X-rays (δ ~ 20nm)
- Hard X-rays (δ ~ 80nm)

X-ray Fluorescence Microprobe

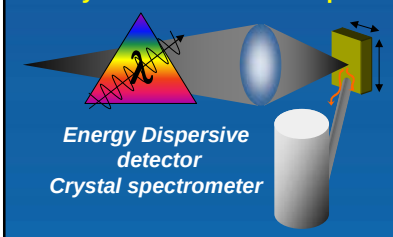

- Hard X-rays (δ ~ 80nm)

Scanning Photo-Emission Microprobe

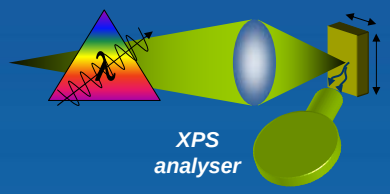

- Soft X-rays (δ ~ 40nm)

Synchrotron based micro-probe techniques

ESRF instruments

X-Ray Fluorescence
- Composition
- Quantification
- Trace element mapping

ID13, ID21, ID22

X-ray Diffraction & scattering
- Long range structure
- Crystal orientation mapping
- Stress/strain/texture mapping

ID11, ID13, ID22

Phase contrast X-ray imaging
- 2D/3D Morphology
- High resolution
- Density mapping

ID21, ID22

Infrared FTIR-spectroscopy
- Molecular groups & structure
- High S/N for spectroscopy
- Functional group mapping

ID21

X-ray spectroscopy
- Short range structure
- Electronic structure
- Oxidation/speciation mapping

ID21, ID22, ID24

Synchrotron based hard X-ray microprobe

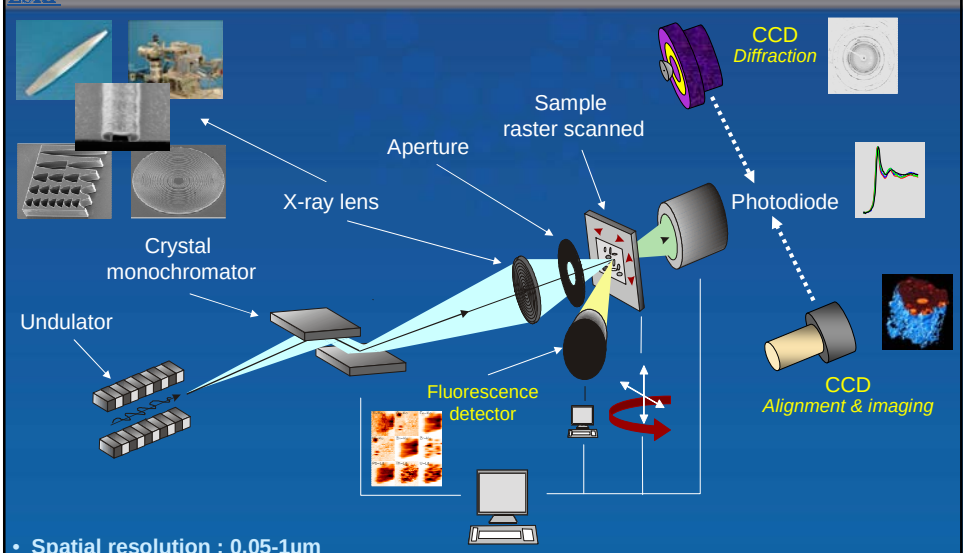

- **Spatial resolution : 0.05-1µm**
- **Spectral resolution : $10^{-2} > \Delta E/E > 10^{-4}$**
- **Averaged flux : $10^{10} – 10^{13}$photons/s/µm^2**

Synchrotron micro-probes

Diffractive lenses

- Resolution determined by probe size and overall stability
- Size of the probe is a convolution of the geometric image of the source and the point spread function of the lens
- Diffraction limited vs aberration limited?
- Coherent illumination required for diffraction-limited resolution but images are not coherent.
- SXMs are coherent (brightness) experiments

Refractive lenses

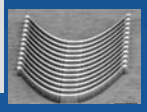

High β_z
25x135µm^2 - 17x208µrad^2

(Secondary) source — 50-250m — ***focus***
< 50x50nm^2

Low β_z
25x930µm^2 - 17x29µrad^2

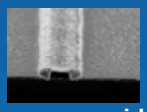

X-ray waveguides

X-ray reflectors

Diffraction limited focusing

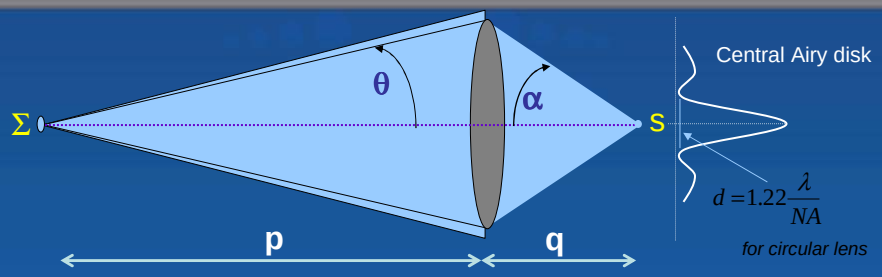

Thin lens equation

$$\frac{1}{f} = \frac{1}{p} + \frac{1}{q}$$

Numerical aperture

$$NA = n\sin\alpha$$

Geometrical demagnification:

$$s_G = \Sigma \times \frac{q}{p}$$

Diffraction limited focusing if $\Sigma \times \theta = \frac{\lambda}{4\pi}$

$$s_{DL} = C\frac{\lambda}{NA}$$

where C=0.61 for a circular aperture

A trade-off

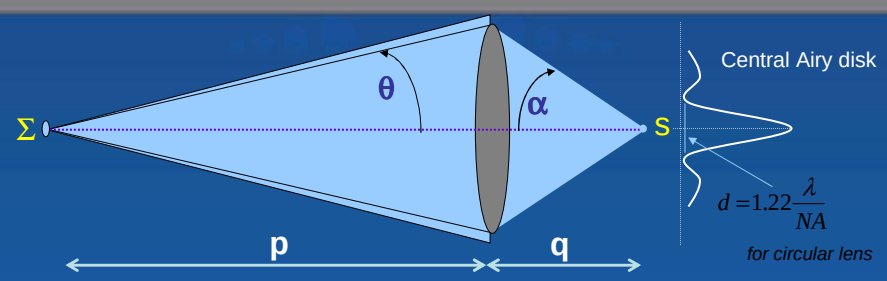

Geometrical demagnification

$$s_G = \Sigma \times \frac{q}{p}$$

Coherent illumination

$$s_{DL} = 1.22\frac{\lambda}{\sin\alpha}$$

Optical aberrations often limit resolution before diffraction limit is reached

- Source size (horiz. vs. vert.)
- Distance source-optics
- Working distance

- Working distance
- Lens aperture
- Beam divergence

Ideal focusing of a point source

- Focusing: equal optical paths source-to-focus
- Ellipse definition: p + q = constant

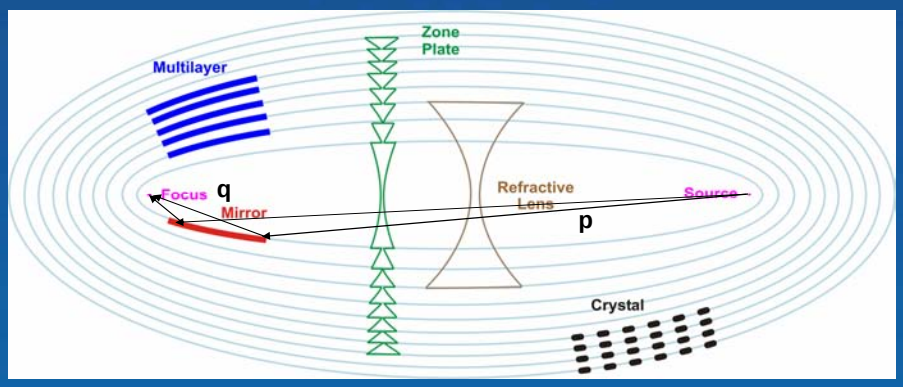

Courtesy C. Morawe (Optics Group)

A fundamental limit: "Liouville's theorem"

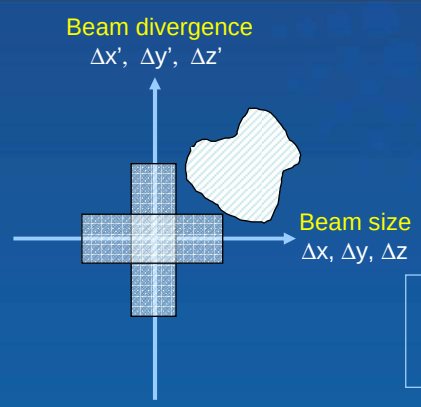

The emittance ε
size x divergence
is constant

$\varepsilon = \Delta_i' \times \Delta_i = const$

- Focussing : Size ↘ and divergence ↗
- Collimating : Size ↗ and divergence ↘

1 - The phase-space density of photons cannot be increased.

2 - In fact, because of absorption and finite efficiency of the optical elements, the phase-space density decreases.

3 - Implications for diffraction experiments.

Undulator beam and spatial modes

- The combined RMS widths due to the one-electron pattern and the electron beam are

$$\Sigma_x = \sqrt{\sigma_x^2 + \frac{\lambda_n L}{4\pi}} \qquad \Sigma_{x'} = \sqrt{\sigma_{x'}^2 + \frac{\lambda_n}{L}}$$

$$\Sigma_y = \sqrt{\sigma_y^2 + \frac{\lambda_n L}{4\pi}} \qquad \Sigma_{y'} = \sqrt{\sigma_{y'}^2 + \frac{\lambda_n}{L}}$$

ACTUAL UNAPERTURED BEAM

- Similarly we can define the full widths as before $\Delta_{\Sigma x} = \sqrt{2\pi}\Sigma_x$ and $\Delta_{\Sigma x'} = \sqrt{2\pi}\Sigma_{x'}$ etc
- The phase space areas in x and y are now $\Delta_{\Sigma x}\Delta_{\Sigma x'}$ and $\Delta_{\Sigma y}\Delta_{\Sigma y'}$
- Of course we could define the beam width and angle by slits - then we could write the phase space areas in x and y as $\Delta_x^{SLIT}\Delta_{x'}^{SLIT}$ and $\Delta_y^{SLIT}\Delta_{y'}^{SLIT}$
- If the phase space area in x is say m_x times bigger than the coherent phase space area then we say that the beam has m_x modes in x and similarly for y - therefore for the unapertured beam we would have

$$m_x = \frac{\Delta_{\Sigma x}\Delta_{\Sigma x'}}{\lambda/2} \quad \text{and} \quad m_y = \frac{\Delta_{\Sigma y}\Delta_{\Sigma y'}}{\lambda/2}$$

From lecture 4, M. Howells

Some source parameters

Electron beam parameters (RMS)

High beta section (even IDs)
- Size H : 415.0µm
- Div. V : 2.9µrad
- Size V : 8.6µm
- Div. H : 10.3µrad

Low beta section (odd IDs)
- Size H : 51.0µm
- Div. V : 2.9µrad
- Size V : 8.6µm
- Div. H : 108.0µrad

Photon source parameters (RMS)

High beta section
- Size H : 415.0µm
- Div. V ~ 13-5µrad (5-40keV)
- Size V : 8.6µm
- Div. H ~ 16-11µrad (5-40keV)

Low beta section)
- Size H : 51.0µm
- Div. V ~ 13-5µrad (5-40keV)
- Size V : 8.6µm
- Div. H : 108.0µrad

Some beam parameters

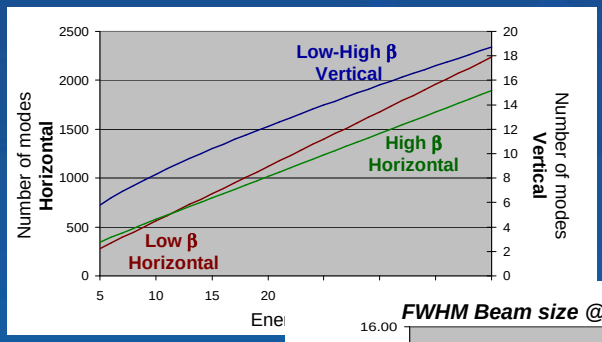

A coherent experiment uses only one mode!!

What about the wasted modes?

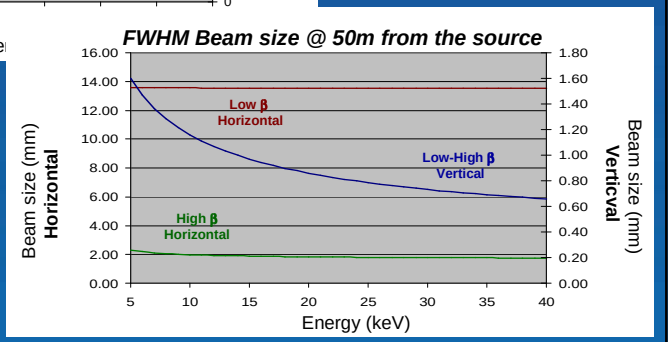

High beta sources provide a slightly more "coherent" beam

Source demagnification : Scheme 1

A "short" beamline with a secondary source

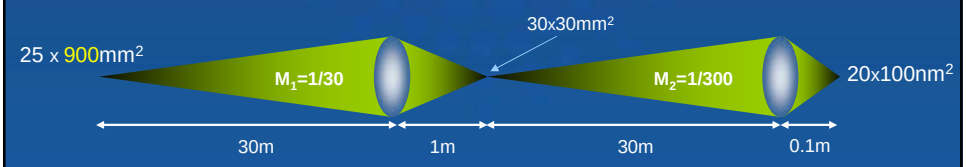

- Compact and stable instrument
- Overfilling of the slits makes the beamline less sensitive to drifts and vibrations
- Optical optimization is possible
- The secondary slit can be used to clean-up the beam (speckles from upstream components)
- Trade-off flux vs. resolution is tunable

- Requires a small pinhole (difficult to produce for hard X-ray?, heat load?, ….)
- Compromises the energy tunability ?

See also lecture 3 (A. Snigirev)

Source demagnification : Scheme 2

Long beamline with a direct source demagnification

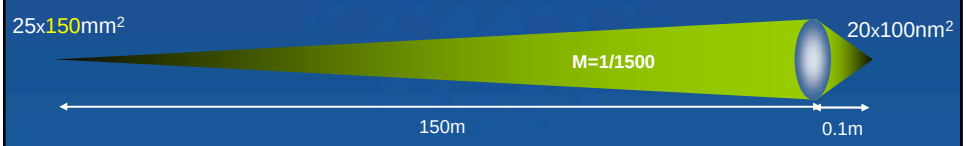

- Exploits the source size (low β or apertured high β)
- Allows long working distance
- Preserves the coherence
- Preserves the energy tunability (spectroscopy)
- Preserves the vertical divergence tunability (diffraction)

- Overall stability
- Flux losses or large aperture optics
- Cost

See also lecture 3 (A. Snigirev)

High energy = very grazing incidence

- Small θ –> Long mirror (> 1m) or small NA
- Off-axis geometry
- Aberrations (spherical aberration, astigmatism, figure errors)

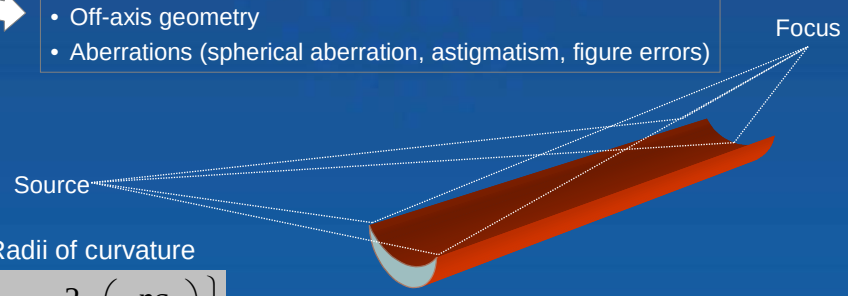

Radii of curvature

$$R_m = \frac{2}{\sin\theta_i}\left(\frac{pq}{p+q}\right)$$

$$R_s = 2\sin\theta_i\left(\frac{pq}{p+q}\right)$$

$$R_s \approx R_m\theta^2$$

$\theta < \theta_c$ ~ 10mrad

$R_s \approx mm$

$R_m \approx km$

$$\theta_{c_{[mrad]}} E_{c_{[keV]}} = 19.83\sqrt{\rho_{[g/cm^3]}}$$

Mirror shapes : $z = \alpha y^2(1+\beta y+\gamma y^2)$, $R_c \sim 1/2\alpha$

- Ellipsoidal : point-to-point focussing

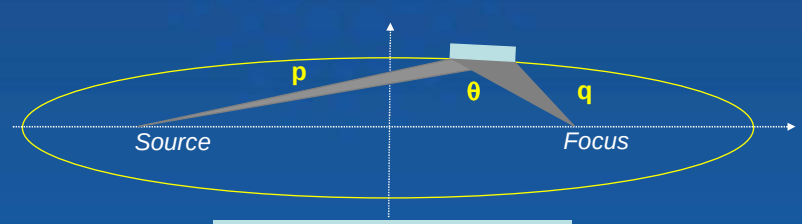

$$\alpha_e = \frac{\sin\theta}{4p}\left(1+\frac{p}{q}\right)$$

$$\beta_e = \frac{\cos\theta}{2p}\left(\frac{p}{q}-1\right)$$

$$\gamma_e = \frac{1}{4pq} + \frac{5\cos^2\theta}{16p^2}\left(1-\frac{p}{q}\right)$$

"ideal" ellipse are extremely difficult to manufactured

J. Susini, Optical Engineering, 34(2) (1995)

Kirkpatrick-Baez geometry

Principle : perpendicular meridian planes
P. Kirkpatrick and A.V. Baez,
"Formation of optical images with X-rays"
J. Opt. Soc. Amer., 38, (1948)

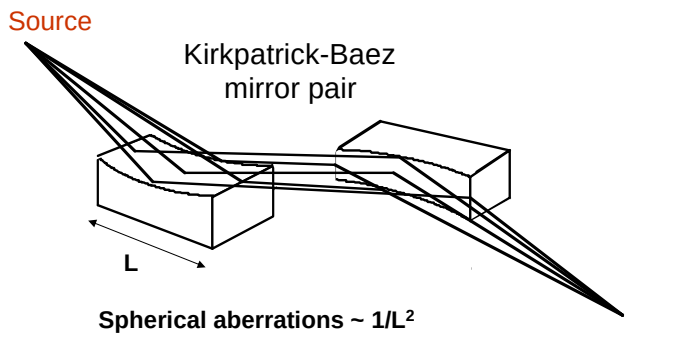

Spherical aberrations ~ $1/L^2$

Multilayer coating :
Bragg angle → shorter mirror or/and larger aperture

Kirkpatrick-Baez system at the ESRF

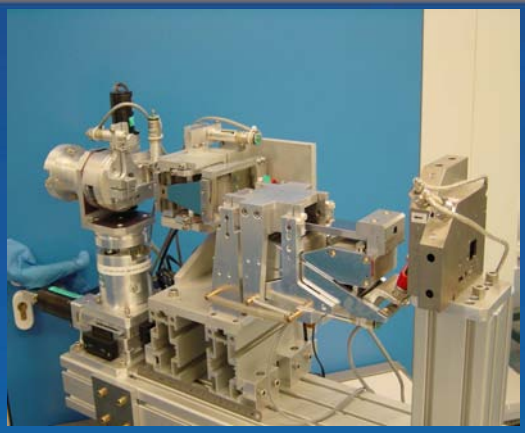

microfocus on ID19 (20.5 keV)

Aperture V X H (µm)	Focus Size FWHM (nm)	Flux Ph/s @90mA
200 X 50	92 X 87	$5\ 10^{10}$
400 X 100	70 X 74	$2\ 10^{11}$
600 X 160	90 X 70	$4.5\ 10^{11}$

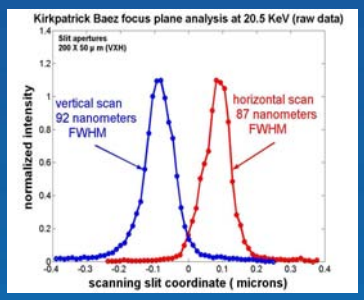

ESRF: 40nm
O. Hignette *et al., AIP Conf. Proc.* 879 (2007)

Spring8: 25nm
H. Minura *et al., APL* 90 (2007)

Fresnel Lenses – Zone Plates

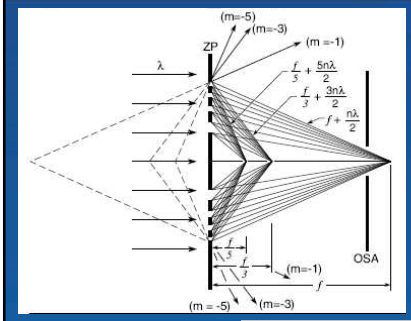

Diffractive X-ray Lenses

Circular transmissive diffraction gratings with radially decreasing line width giving focusing effect

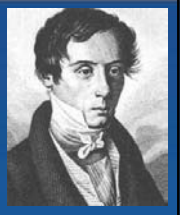

Augustin-Jean Fresnel
1788-1827

Alternate 'zones' modify phase/amplitude of incident wavefront: for material of thickness, t, wavelength, λ, refractive index $1-\delta-i\beta$, phase shift, $\Delta\phi$, is:

$$\Delta\phi = \frac{2\pi\delta t}{\lambda}$$

For X-rays:

Baez (1952), Schmahl (1969), Kirz (1971), Niemann (1974)

Fresnel zone plates: a Gabor hologram of a point object

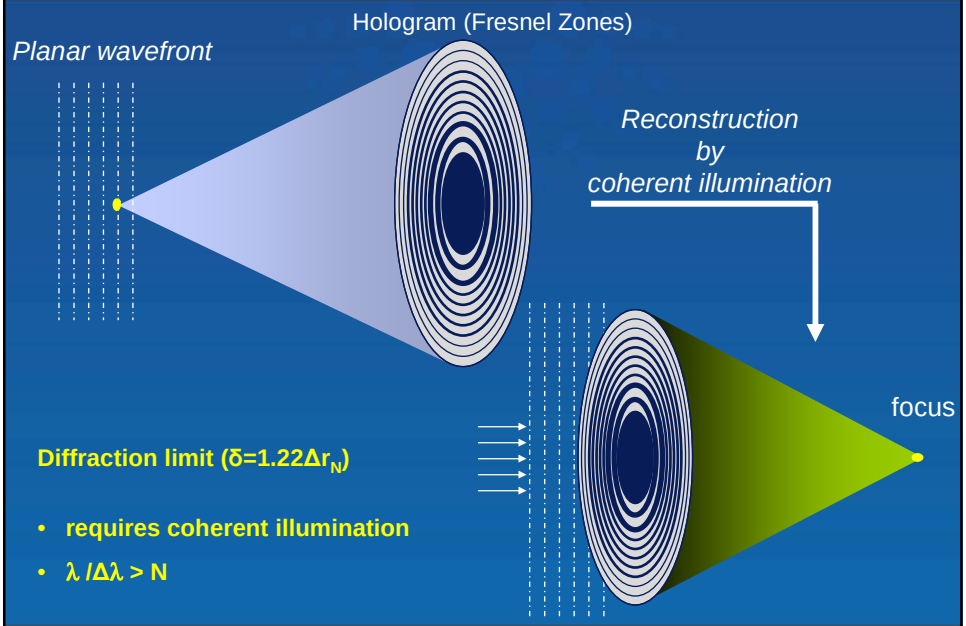

Diffraction limit ($\delta=1.22\Delta r_N$)

- **requires coherent illumination**
- **$\lambda/\Delta\lambda > N$**

Fresnel Zone Plates

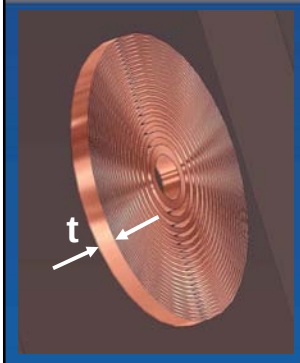

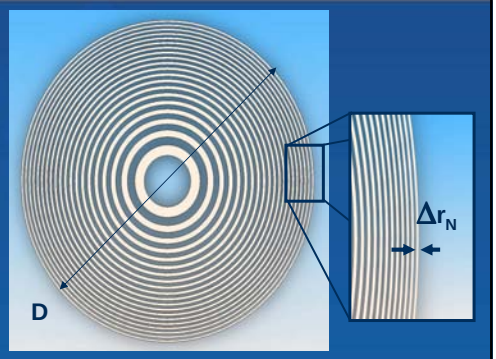

- Resolution: $\delta_m = 1.22 \frac{\Delta r_N}{m}$
- Focal length: $f_m = \frac{D\,\Delta r_N}{m\,\lambda}$
- Depth of focus: $DOF = \pm \frac{4\,\Delta r_N^{\,2}}{m\,\lambda}$

- m=1
- Δr_N=50nm
- D=100µm

2mm @500eV
40mm@10keV

8µm @500eV
160µm@10keV

Soft X-ray zone-plates

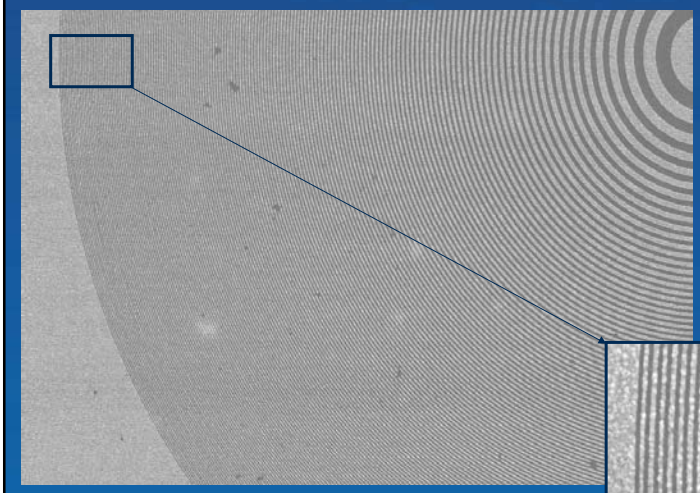

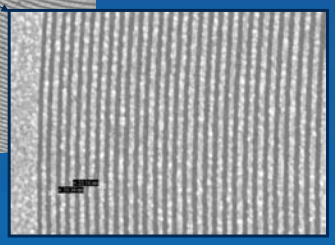

- Δr_N = 25 nm
- D = 63 µm
- N = 618 zones
- f = 650 µm
- NA = 0.05
  @ λ = 2.4 nm

- Δr_N = 15 nm
  W. Chao *et al.*, *Nature* 435 (2005)

E. Anderson, ***C**enter for **X**-**R**ay **O**ptics*, LBNL, USA

Zone plate aspect ratio

structure height, t, critical for efficiency, Δr_N for resolution

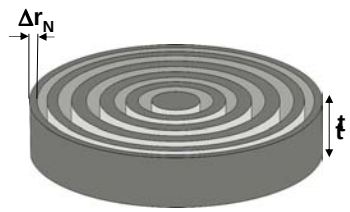

Material	t (µm)	ε (%)
E=0.5keV		
Ge	0.28	16
Ni	0.25	24
E=2.0keV		
Ni	0.60	25
Au	0.45	24
E=8.0keV		
Ta	1.70	32
W	1.50	33

Aspect ratio for Δr_N=50nm

Practical limit for small Δr_N is ~ 10-15:1

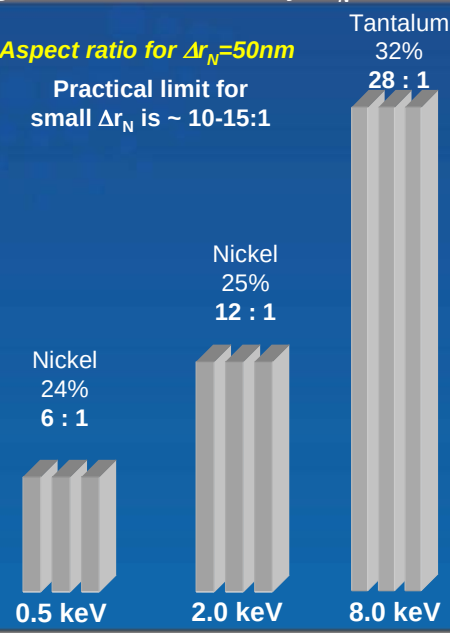

Fresnel zone-plates: several strategies

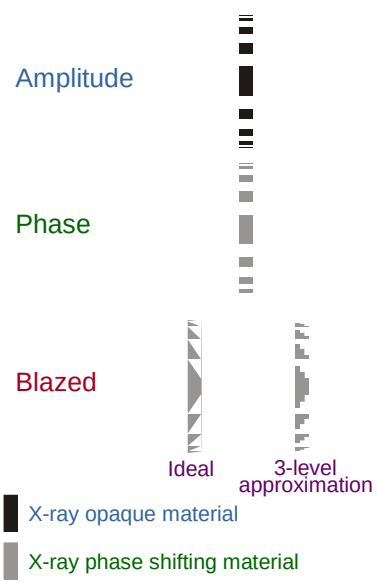

- ***Grating with equal lines and spaces***

$$\varepsilon_m = \frac{1}{m^2\pi^2}\left(1+e^{-2K\Phi}-2e^{-K\Phi}\cos\Phi\right)$$

$$K=\frac{\beta}{\delta} \text{ and } \Phi=\frac{2\pi\delta}{\lambda}$$

m = ±1, ±3, ±5,….

- **Amplitude** : Opaque zones (K→ ∞)

ε_1 ~ 10% and ε_3 ~ 1%

- **Phase :** weak absorbing and phase reversal zone (K→0 and Φ = π)

ε_1 ~ 40 %

$$\varepsilon_m(p) \approx \frac{1}{m^2}\left(\frac{\sin\left(\pi/p\right)}{\pi/p}\right)^2$$

$\varepsilon_1(2)$ = 40.5%
$\varepsilon_1(3)$ = 68.5%
$\varepsilon_1(4)$ = 81.2%

Blazed zone plate: 3 level lens

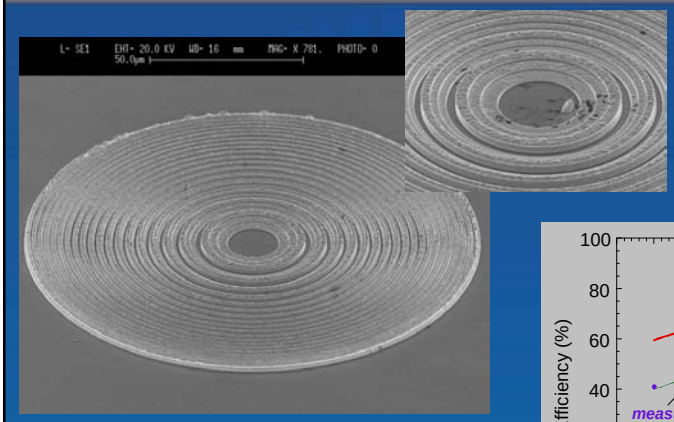

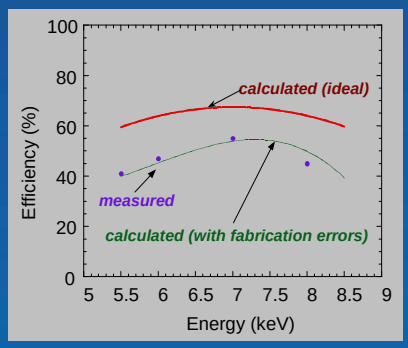

- material : Nickel
- diameter : 150µm
- ΔR_N : 150nm

→ 7 keV : ε ~ 57%

E. di Fabrizio *et al.*, *Nature* 401 (1999)

Rejection of the unwanted diffraction orders

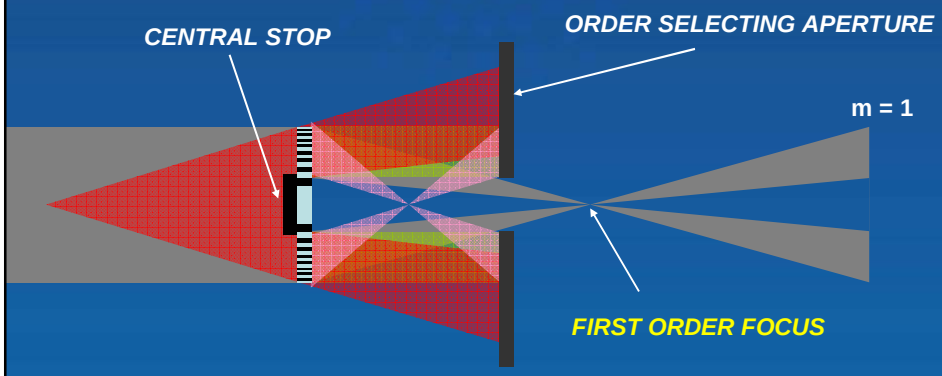

Zone-plate based SXM = Central stop + ZP + OSA

SXM – ID21 – Old version

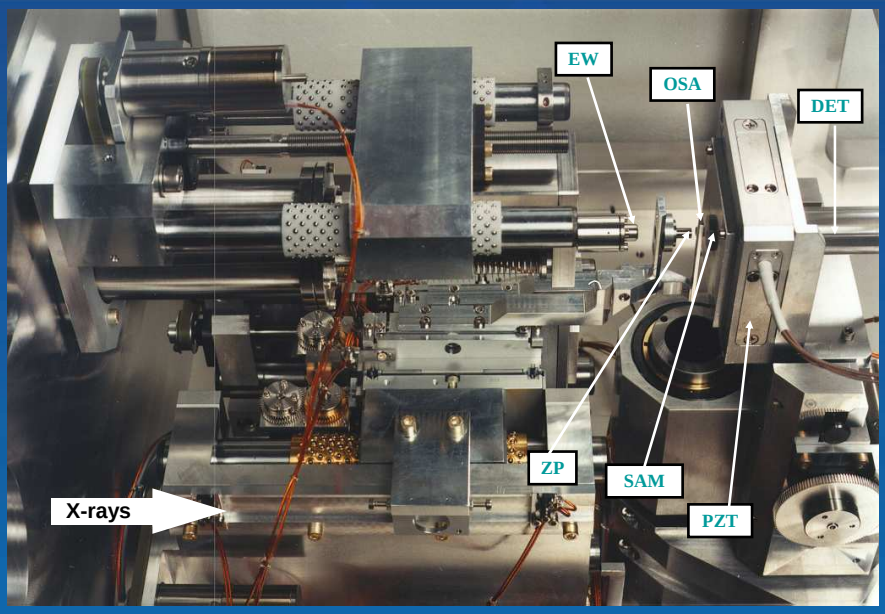

Multilayer Laue Lenses

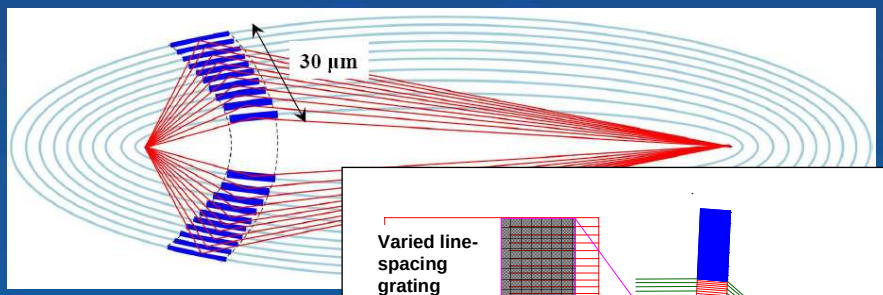

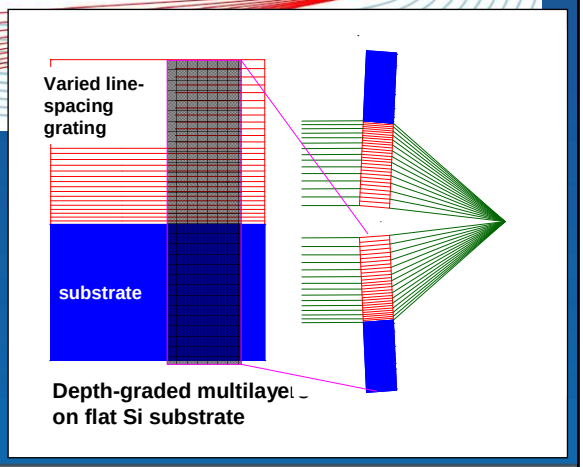

- Deposit varied line-spacing grating on flat substrate (thinnest structures first)
- Section to 5-20 µm thickness (high aspect ratio structure)
- Assemble two into a single device (MLL)

H. C. Kang et al., Phys. Rev. Lett. 96 (2006)

Tentative of comparison

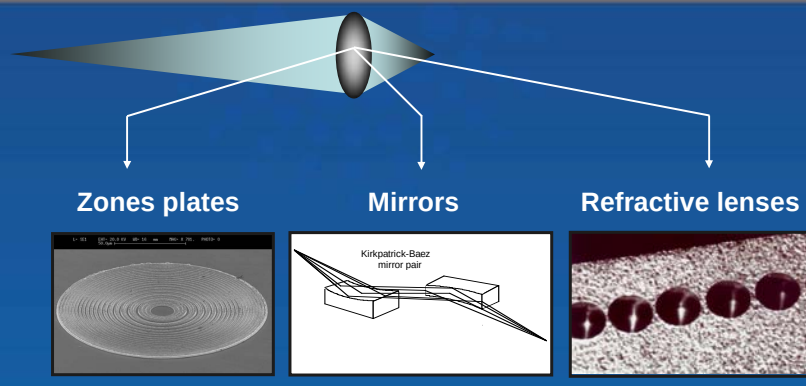

	Zones plates	Mirrors	Refractive lenses
• Resolution	++++	+++	+++
• Achromaticity	-(-)	+++(+)	--(-)
• Efficiency	+	+++(+)	++
• Imaging (MTF)	++++	++	+++

X-ray Fluorescence: a brief reminder

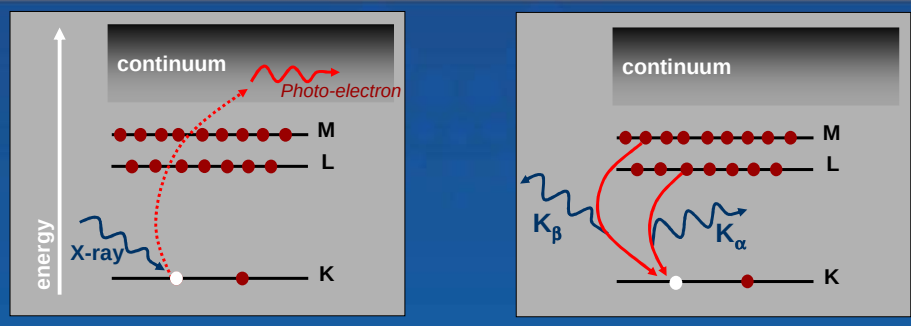

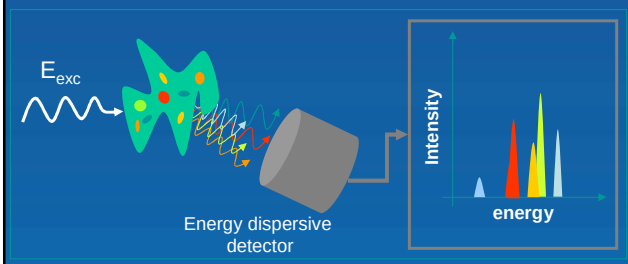

- ✓ Element specific
- ✓ Co-localization
- ✓ Quantification

XRF on synchrotron beamline = low detection limit

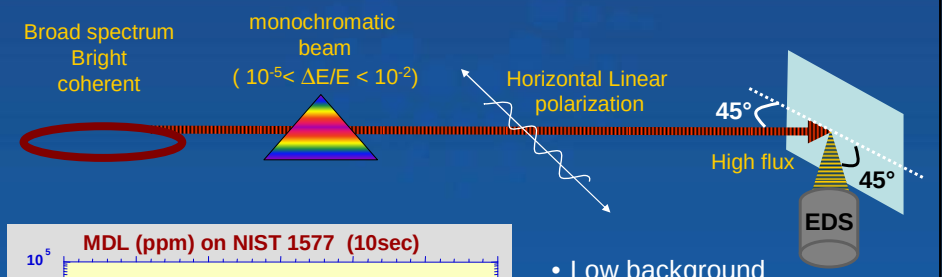

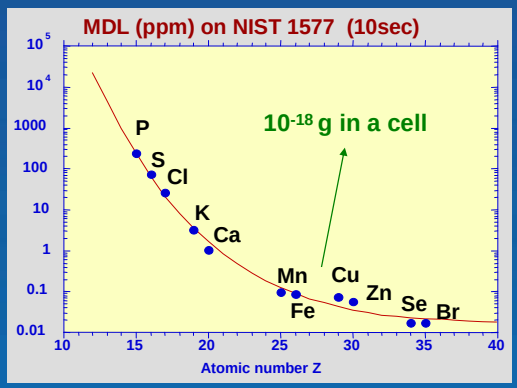

- Low background
- Tunable energy (XANES)

Only a few degrees collection angle!

Detector developments

Dwell time < 100ms

μ-XRF in Trichomes of Arabidopsis Thaliana

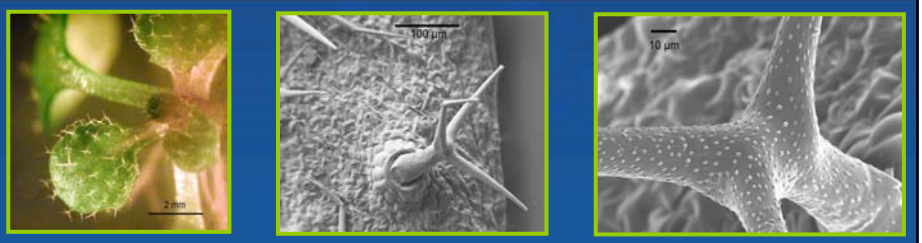

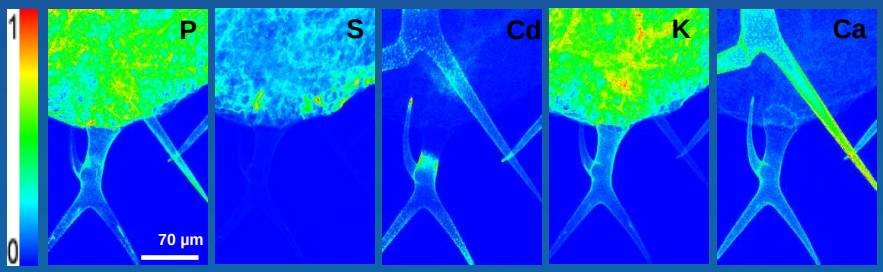

E_{ex}: 5.8 keV, probe size: 0.3x0.2μm², dwell time: 800 ms/pixel.

M.P. Isaure *et al.*, *Biochimie*, 88, 2006

Fluorescence tomography (3D-µXRF)

Pixel- by-pixel acquisition

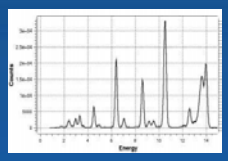

Sinogram(s)

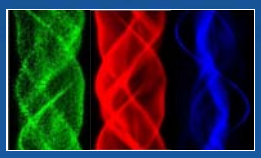

2D-Slice or 3D-Volume

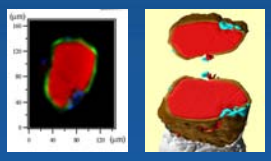

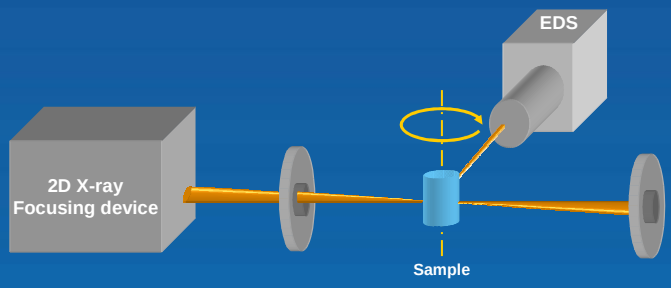

Fluorescence tomography (3D-µXRF)

Pixel- by-pixel acquisition

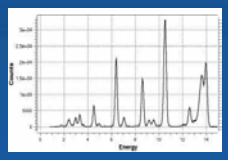

Sinogram(s)

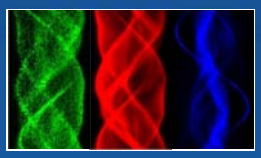

2D-Slice or 3D-Volume

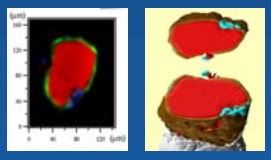

- **The reconstruction problem is far more difficult compared to transmission tomography**
  - **self absorption corrections**
  - **$\mu(E_a, x)$ is a priori unknown**
  - **weak fluorescence signal for light elements**

ESRF Lecture Series on Coherent X-rays and their Applications,
Lecture 6 - Jean Susini

Fluorescence tomography (3D-µXRF)

Pixel- by-pixel acquisition

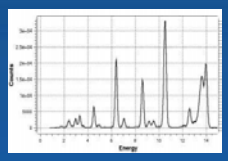

Sinogram(s)

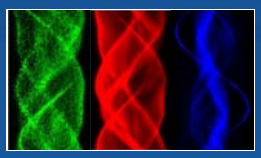

2D-Slice or 3D-Volume

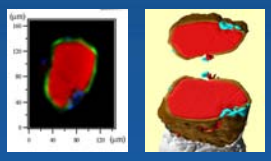

Algorithmic solution:

Optimal estimation of attenuation maps by combination of transmission, fluorescence and Compton tomographies

- B. Golosio *et al.*, *J. Appl. Phys.* 94(1) (2003)

Geometrical solution:

Collimation of the detection angle to define a voxel: confocal geometry

- B. L. Vincze et al., *Anal.Chem.*, 76(22) (2004)

Combining several signals

Compton tomography ($\sigma_{Compton}$~Z)

➢ ***Electronic density* maps**

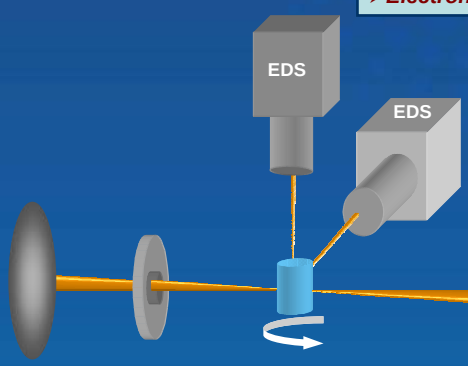

Fluorescence tomography

➢ ***Elemental* composition maps**

Absorption tomography (σ_{photo}~Z^4)

➢ ***Absorption coefficient* maps**

Integration of the information

Absorption + Compton + Fluorescence

↓

QUANTIFICATION

B. Golosio *et al.*, *J. Appl. Phys.* *94*(1) (2003) B. Golosio *et al*, *APL* 84 (2004)

Single Fly Ash Particle

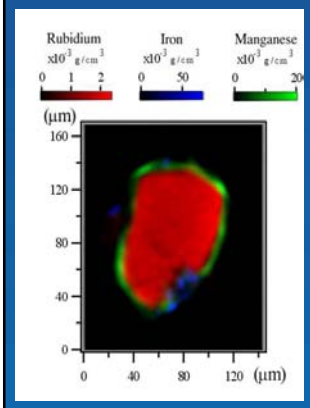

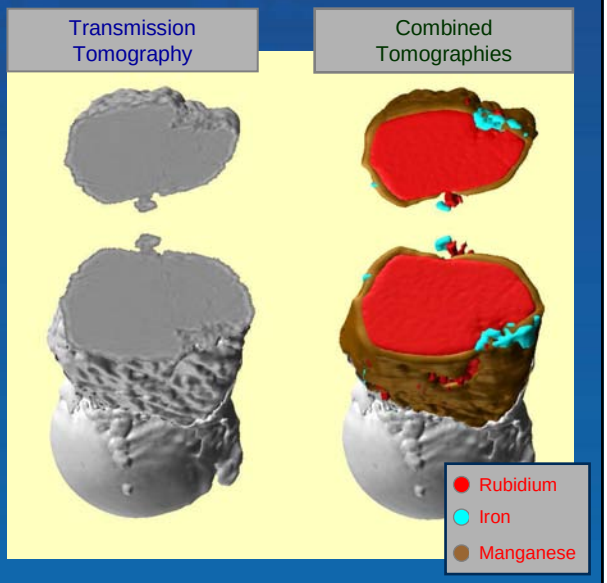

ESRF Lecture Series on Coherent X-rays and their Applications, Lecture 6 - Jean Susini

B. Golosio *et al*, *Applied Phys. Letters*, 84 (2004)

XRF Tomography – "confocal geometry"

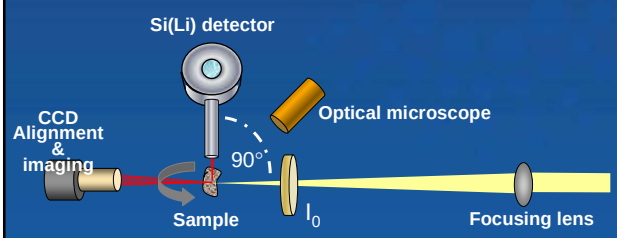

ESRF - ID18F

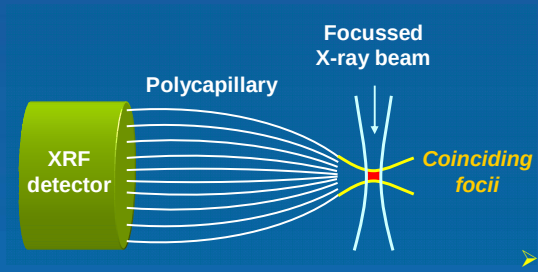

- Spatial resolution: 5-10µm

ESRF Lecture Series on Coherent X-rays and their Applications, Lecture 6 - Jean Susini

L. Vincze *et al.*, *Anal.Chem.* 76(22) (2004)

From 3D-confocal XRF to quantification

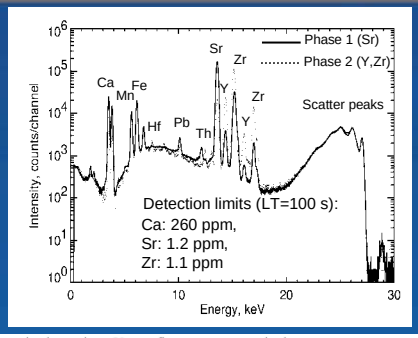

Quantitative micro X-ray fluorescence analysis

Element	Larnite (β-Ca_2SiO_4) (ppm)	$CaSiO_3$-walstromite (ppm)	Th-rich phase (ppm)
Ca	29.6 ± 5.9%	18.6 ± 5.4%	1.2 ± 0.4 %
Mn	391 ± 25	386 ± 26	47 ± 10
Fe	254 ± 13	220 ± 16	114 ± 11
Sr	431 ± 3	48 ± 1	92 ± 3
Y	9 ± 1	61 ± 2	22 ± 3
Zr	35 ± 1	233 ± 2	59 ± 2
Hf	<DL	3 ± 1	1 ± 1
Pb	7 ± 2	2 ± 1	3 ± 1
Th	<DL	1 ± 1	51 ± 2
U	<DL	4 ± 1	6 ± 2

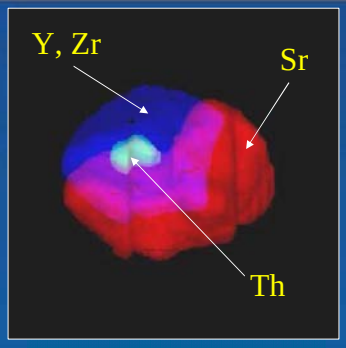

unusual high Ca concentration

"Ca-rich lithology in the Earth's deep (> 300 km) convecting mantle "

B. Vekemans *et al.*, *JAAS.* 19(10) (2004) F.E. Brenker *et al.*, *EPSL* 236 (2005)

X-ray Absorption Near Edge Spectroscopy (XANES)

Electronic transitions to bound states, nearly bond states or continuum

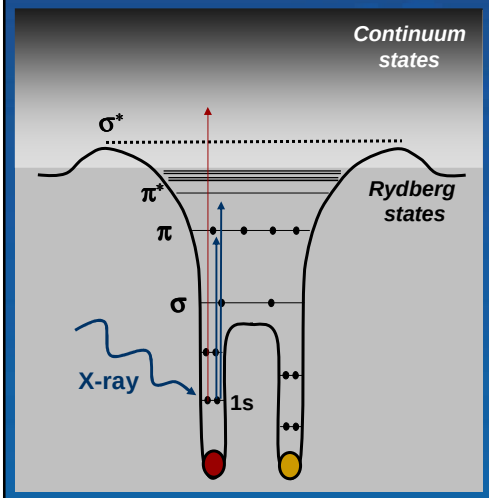

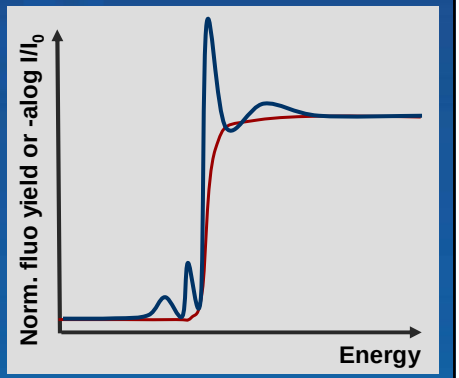

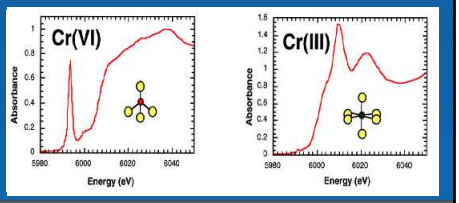

Chromium chemical mapping in cells

Micrograph

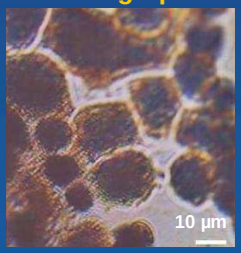

Potassium

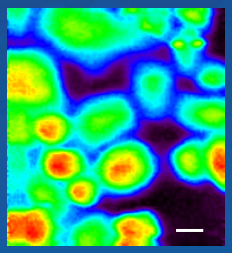

Cr (total)

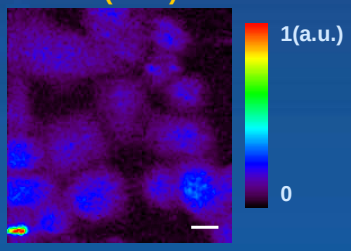

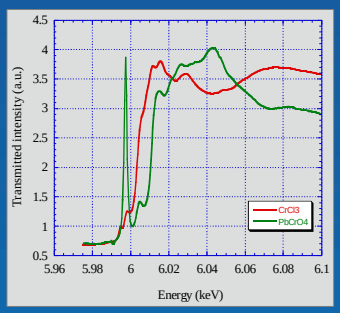

Cr(VI)

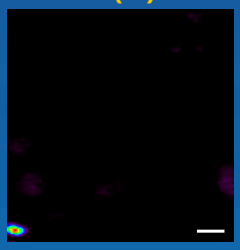

ESRF Lecture Series on Coherent X-rays and their Applications, Lecture 6 - Jean Susini

R. Ortega *et al.* , *Chem. Res. Toxicol.*, 5, (2005)

Absorption and Phase contrasts

Refractive index n for X-ray wavelengths: n ~ 0.999999

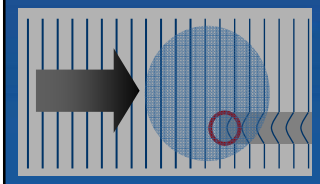

$$n = 1 - \delta + i\beta$$

phase

amplitude

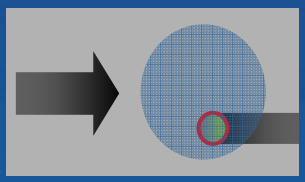

Phase contrast

~ 1 / E

Absorption contrast

~ 1 / E^3

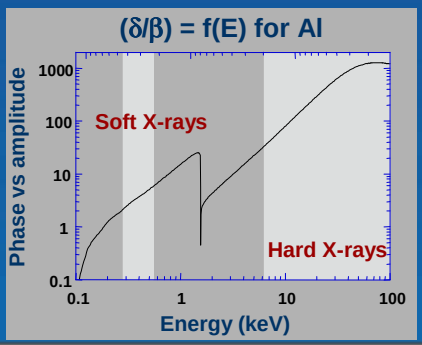

ESRF Lecture Series on Coherent X-rays and their Applications, Lecture 6 - Jean Susini

See lecture 5 - P. Cloetens

X-ray microscopy techniques using phase shifting

		SXM	TXM
Bonse / Hart (1968)	**X-ray interferometer** based on double crystal in Laue geometry keV photons	X	X
Schmahl et.al (1993)	**Zernike phase contrast** with phase shifting annular plate in back-Fourier plane of imaging objective soft X-rays & keV photons)	X	√
Morrison et.al (1996)	**Differential phase contrast** using a quadrant detector similar to SEM soft X-rays & keV photons	√	X
Polack / Joyeux (1995) Kaulich / Wilhein (2002)	**Differential phase contrast** using Young type slits or a Fresnel bi-mirror Using 2 zone-plates soft X-rays (keV photons)	√	√

Phase contrast in SXM ?

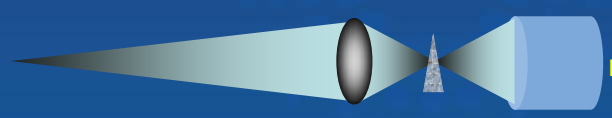

Intensity variation ?

Phase gradients
due to material inhomogeneities or thickness variations

2 options

Differential Phase Contrast
(DPC)

Beam deflection
+
Configured detector
=
intensity variation

Differential Interference Contrast
(DIC)

Phase effects
+
interference fringes
=
intensity variation

DPC: SXM and configured detectors

Phase gradients due to material inhomogeneities or thickness variations cause a deflection of the microprobe beam

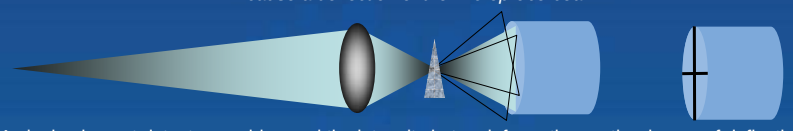

- A single element detector would record the intensity but no information on the degree of deflection
  → *Absorption only*
- If the detector is split into several pixels, the beam deflection leads to intensity variation can detected
  → *Phase information* can be extracted.

Reciprocity Principle

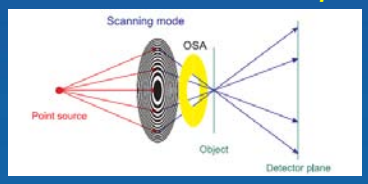

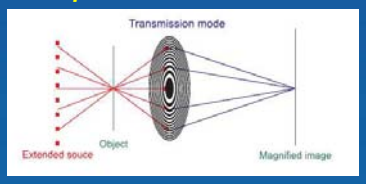

- STXM and TXM imaging modes can produce equivalent image contrast
- The roles of source and detector can be interchanged
- STXM mode allows some imaging conditions to be realized more easily than in TXM mode,
- … and vice versa !

See also Lecture 4 (M. Howells)

DPC and fast-readout CCD array detector

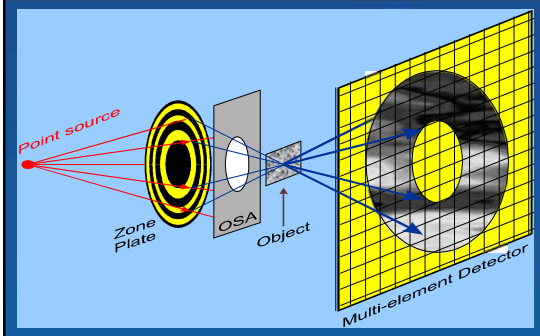

- 80x80pixels
- Spreads signal across many detector elements
- Extends the dynamic range for which photon counting is possible.
- Allows flexible choice of imaging modes (with simultaneous absorption, phase and dark field contrast)

W. Eaton et al., *AIP Proceedings* 507 (2000)

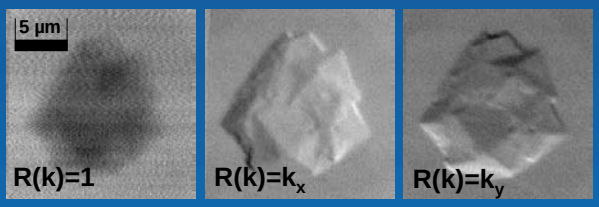

CVD Diamond
ID21
3.3keV
100nm pixel size

G.R. Morrison et al., *Journal de Physique IV* 104 (2002)

Configured segmented detector

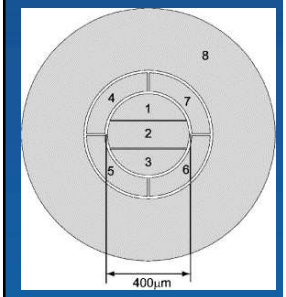

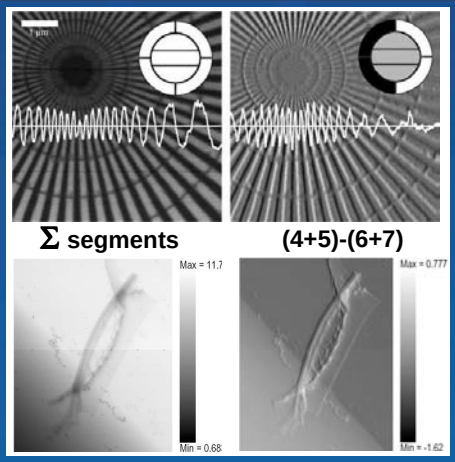

Ge siemens star
525eV
X1A microscope
NSLS

Diatom
10keV
Beamline 2-ID-E
APS

- M. Feser et al., *NIM A.* 565 (2006)
- B. Hornberger et al. *Ultramicroscopy 107(8)* (2007)
- M.D. de Jonge et al., *Microsc Microanal* 13(2) (2007)

Differential Interference Contrast (DIC)

Visible light microscopy

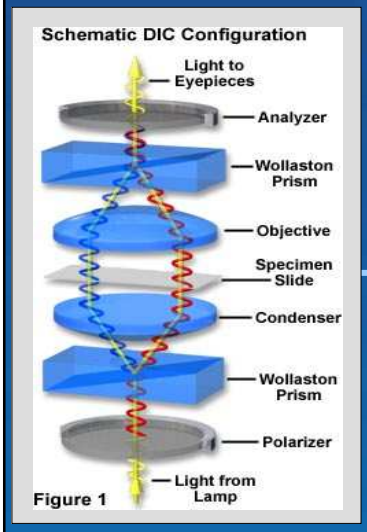

G. Nomarski, 1960

The image of DIC microscopes is formed from the interference of two mutually coherent waves with lateral displacements (shear) of the order of the minimum size of the imaged structure and are phase-shifted relative to each other

The intensity distribution in measured DIC images is given by a non linear function of the spatial gradient of a specimen's optical path length distribution along the direction of shear

- Two plane polarizers are involved, one before the condenser and one after the objective.
- Birefringent prisms act on the plane polarized light first to split the beam in two, and later to recombine the two beams.

Differential Interference Contrast (DIC)

Visible light microscopy

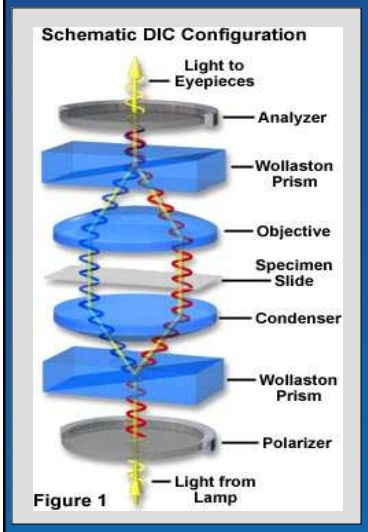

G. Nomarski, 1960

X-ray microscopy

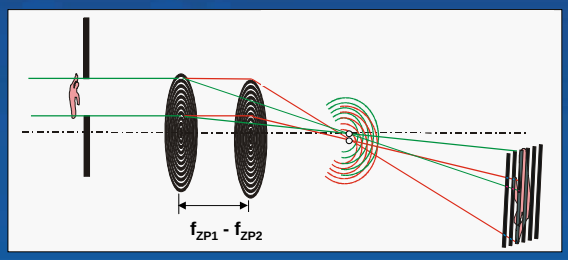

- T. Wilhein *et al.*, *Appl. Phys. Lett.* 78(14), (2001)
- T. Wilhein *et al.*, *Optics Communication* 193, (2001)
- B. Kaulich *et al.*, *J Opt Soc Am A* 19(4), (2002)
- B. Kaulich *et al.*, *Optics Express*, 10(20) (2002)
- E. Di Fabrizio *et al.*, *Optics Express*, 11(19) (2003)

X-ray Differential Interference Contrast (X-DIC)

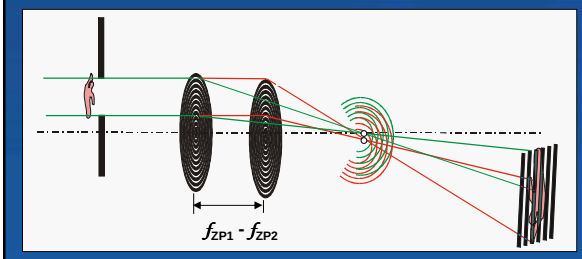

- *Shear of wave front division or distance of Airy disks in focal plane is smaller than optical resolution ("differential")*

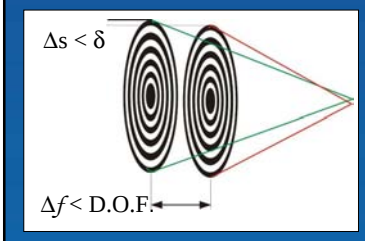

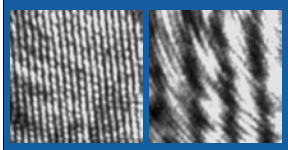

λ=0.3nm

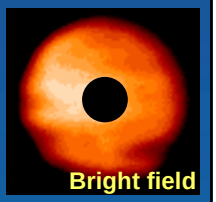

- Distance Δf of both ZPs smaller than depth of field
- Displacement Δs smaller than resolution δ

X-ray Differential Interference Contrast (DIC)

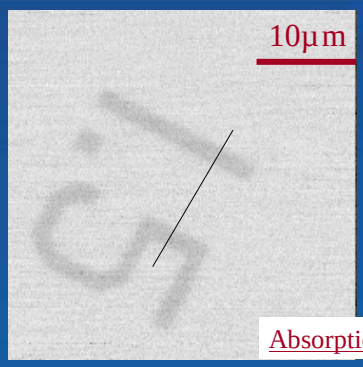

PMMA test object
ID21
E=5keV

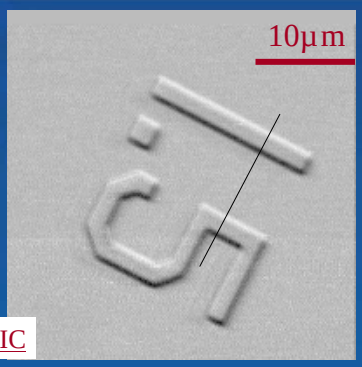

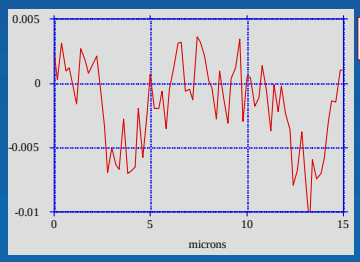

C~ 1%

C > 28%

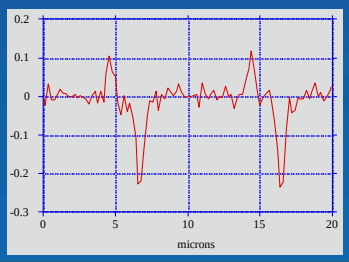

B. Kaulich *et al.*, *J Opt Soc Am A* 19(4), (2002)

X-ray Differential Interference Contrast (X-DIC)

Development of multi-spot zone plates by reconstruction
of the hologram of a plane wave and several spherical waves
(TASC-INFM, Trieste, Italy)

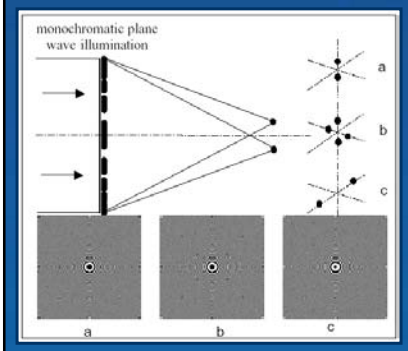

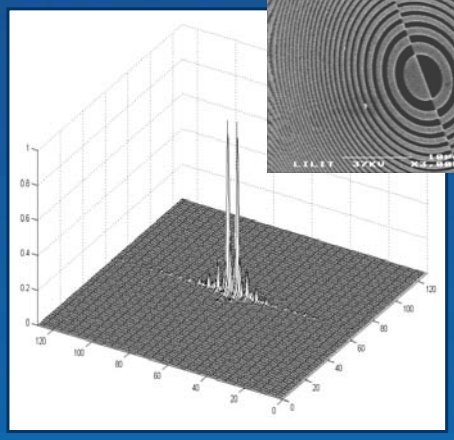

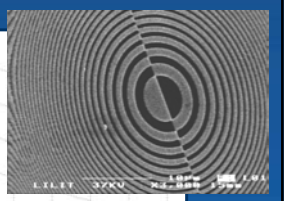

E. di Fabrizio *et al.*, *Optics Express*, 11(19) (2003)

X-ray Differential Interference Contrast (X-DIC)

Cell membranes of maize plant cells

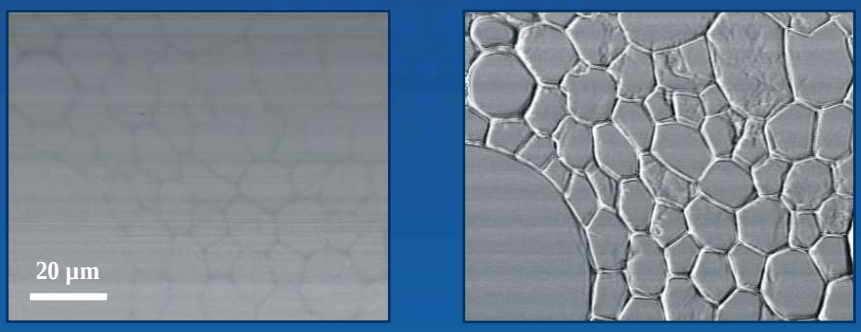

Absorption | X-DIC (phase)

- E = 5.8keV (λ=2.1Å)
- Dwell time: 50 ms/px
- Probe size: 0.6x0.7µm²

unpublished

X-DIC+XRF microscopies = Quantification?

µ-XRF | **X-DIC**

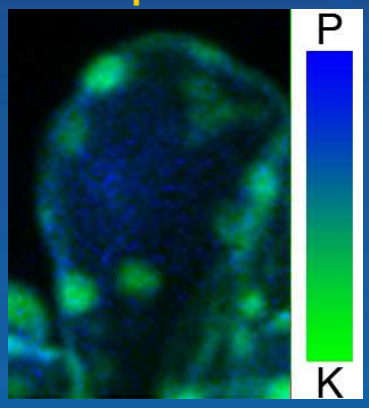

Arabidopsis thaliana

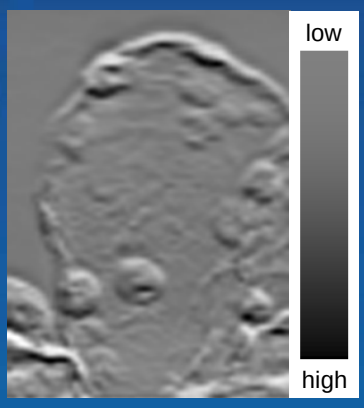

5µm

Intensity maps → ← Density+thickness map

↓

quantification

Multi-keV X-ray microscopy

❖ **Geometry**
- Spatial res.: 1000nm → 30nm
- Field of view: variable
- Depth of field > 10µm
- Working distance > 20mm

→ Multi-scale (meso-scale)
→ Tomography
→ *Sample environment (cryo)*
In-situ

❖ **Contrast mechanisms**
- Phase contrast
- X-ray fluorescence
- Micro-spectroscopy (XANES)

→ Lower exposure dose
→ *Trace element detection*
Quantitative XRF analysis
→ *Chemical state specificity*

❖ **Sample**
- Hydrated-frozen
- Thick
- Minimum preparation

→ Cryo is mandatory
→ No labeling
→ No sectioning

Needs for a multi-modal approach